Effect of ship hull form on the resistance penalty from biofouling

BIOFOULING, 2018
VOL. 34, NO. 3, 262–272
https://doi.org/10.1080/08927014.2018.1434157

Taylor & Francis
Taylor & Francis Group

Effect of ship hull form on the resistance penalty from biofouling

Dinis Oliveira[a], Ann I. Larsson[b] and Lena Granhag[a]

[a]Department of Mechanics and Maritime Sciences, Chalmers University of Technology, Gothenburg, Sweden; [b]Department of Marine Sciences, University of Gothenburg, Tjärnö – Strömstad, Sweden

ABSTRACT

Hull biofouling is a well-known problem for the shipping industry, leading to increased resistance and fuel consumption. Considering that the effects of hull form on resistance are known to be higher for a less slender hull, it is hypothesised in this paper that the effect of biofouling roughness on resistance is also dependent on the hull form. To test this hypothesis, previously reported full-scale numerical results on a containership are re-analysed. Form effects on roughness penalties, corresponding to $K_{\Delta CT} = 0.058 \pm 0.025$, are observed at a low speed (19 knots, $Re_s = 2.29 \times 10^9$), which are however cancelled out by traditionally neglected roughness effects on wave-making resistance at a higher speed (24 knots, $Re_s = 2.89 \times 10^9$). It is concluded that hull form effects on biofouling penalties can be significant at low speeds, though not generalisable for higher speeds, namely when wave-making resistance corresponds to ≥ 29% of total resistance.

ARTICLE HISTORY
Received 16 June 2017
Accepted 25 January 2018

KEYWORDS
Turbulent boundary layer; frictional resistance; roughness; ship resistance; hull form factor

Introduction

In today's globalised world, about 90% of world trade relies directly on commercial shipping (ICS 2017). Sea transport is at present dependent on fossil fuels as energy sources and contributes to ~3% of global CO_2 emissions (IMO 2014), thus raising economic, environmental and societal issues.

A well-recognised way to avoid fuel penalties, and at the same time reduce emissions of greenhouse gases and air pollutants, is by making the hull as smooth as possible, and retaining smoothness during vessel operation. The ideal situation would be a hydraulically smooth hull. The required roughness height k_t for a smooth hull is however prohibitively low, usually < 20 μm, which is much lower than typical out-of-dock roughness of ~150 μm (Lackenby 1962; Johansson 1984; Schultz 2007). Therefore, ship operators must find a balance between voyage costs, ie increase in fuel costs or reduced speed, and maintenance costs, ie hull conditioning, cleaning and repainting. In order to achieve this, a practical method to accurately determine increased resistance due to hull roughness is required.

Currently, the most common methods available for determining increased propulsion power due to hull roughness include sea trials and voyage performance monitoring (Andersen et al. 2005; Munk et al. 2009; ISO 2016). However, sea trials are only performed sporadically, due to time and environmental constraints, whereas voyage performance data suffer from high uncertainty due to changes in draft and trim, weather conditions (wind and waves), sea currents, temperature and salinity (Munk et al. 2009). Thus, most of the previous studies on hull penalties have relied on laboratory-scale experimental results and extrapolation methods to the full-scale ship (Leer-Andersen and Larsson 2003; Schultz et al. 2011; Monty et al. 2016).

In this paper, it is hypothesised that the hull form can affect the prediction of full-scale penalties based on laboratory-scale friction results, since results from the laboratory are often scaled up to the full-scale ship using flat plate frictional resistance. Previously published computational fluid dynamics (CFD) results for a containership (Demirel et al. 2017) are re-analysed here in order to determine the extent to which the form of the hull can affect the penalty due to hull roughness. The theoretical background is developed in the next sub-section.

Roughness effects at laboratory and full scale

Hull roughness is caused by mechanical processes on the hull surface (eg sand-blasting treatment on steel prior to painting, mechanical damage to the coating, and

CONTACT Dinis Oliveira dinis.oliveira@chalmers.se

occurrence of corrosion) and it is significantly increased by the occurrence of biofouling, ie the growth of marine organisms on the hull surface (Schultz 2007).

From a smooth to a hydraulically rough surface, frictional resistance, ie the tangential force caused by viscous flow over the surface, increases due to protrusion of roughness elements above the laminar viscous sub-layer (Larsson and Raven 2010a). This results in a downward shift in velocities measured at a range of distances from the hull (Lewthwaite et al. 1984). Thus, the following equation applies for the velocity profile within the so-called logarithmic region of the boundary layer (Walker 2014):

$$u^+ = \frac{1}{\kappa} \ln\left[(y+\varepsilon)^+\right] + C - \Delta U^+ \quad (1)$$

where velocity u, the component tangential to the hull, made dimensionless by dividing by the wall shear velocity u_τ ($u^+ = u/u_\tau$), is given as a function of the distance from the hull y, with wall origin error ε, also given in viscous units: $(y+\varepsilon)^+ = (y+\varepsilon)u_\tau/v$. Both the origin error ε and the roughness function ΔU^+ are variables dependent on the roughness of the wall.

Determination of the wall shear velocity, $u_\tau = (\tau_w/\rho)^{1/2}$, is a fundamental step for determining the effects of roughness on frictional drag in wall-bounded turbulent flows. The value of u_τ is used in scaling of the velocity profile, as presented in Equation 1. The roughness function ΔU^+ (Equation 1) then corresponds to a downward shift in velocity profile in the presence of a rough wall: ΔU^+ is zero for a hydraulically smooth surface and > 0 for transitionally and fully rough surfaces. The roughness function ΔU^+ has been determined for different types of roughness (Figure 1), including uniform sand roughness (Nikuradse 1933; Cebeci and Bradshaw 1977) and antifouling coatings (Johansson 1984; Schultz 2004; Candries and Atlar 2005). As shown in Figure 1, ΔU^+ can be collapsed for disparate roughness geometries in the fully rough regime (ie high Reynolds number) by use of the so-called equivalent sand-roughness height k_s. However, there is no universal curve for the transitionally rough regime, ie a curve applicable to all roughness geometries at moderate values of Reynolds number k_s^+ (Bradshaw 2000). Therefore, ΔU^+ must be experimentally determined for each new type of roughness (Grigson 1987). Using ΔU^+ curves (Figure 1), extrapolation methods enable determination of ship-scale increased resistance for a given hull roughness condition (Schultz 2007). Alternatively, ΔU^+ can be used as an input to CFD codes for calculating ship resistance (Leer-Andersen and Larsson 2003; Demirel et al. 2014, 2017).

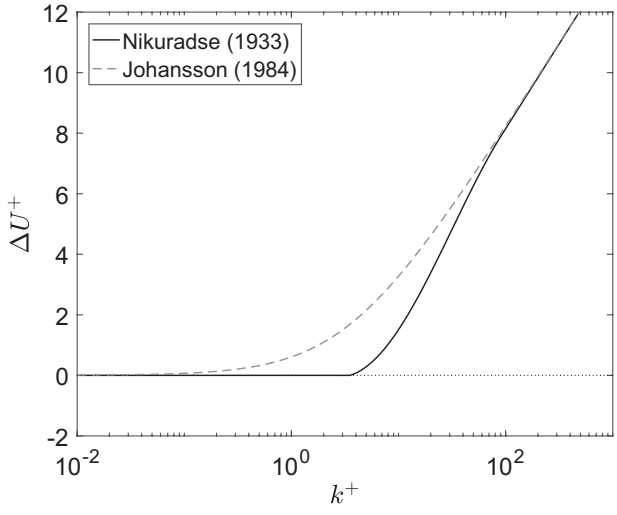

Figure 1. Two examples of roughness function ΔU^+: Nikuradse's uniform sand roughness function (Nikuradse 1933; Cebeci and Bradshaw 1977) and Colebrook-type roughness function (Johansson 1984).

The effect of roughness on ship resistance has been studied extensively within the past 100 years. Increased frictional resistance is usually pinpointed as the primary effect, corresponding to increased tangential forces acting on the hull (Woods Hole Oceanographic Institute 1952; Schultz 2007). When analysing the components of ship resistance R_T, frictional resistance R_F is separated from pressure resistance R_P, each representing the area integral of tangential and normal components of force, respectively, projected in the direction opposing the ship's movement:

$$R_T = R_F + R_P \quad (2)$$

or, using dimensionless coefficients:

$$\frac{R_T}{1/2\rho U^2 S} = \frac{R_F}{1/2\rho U^2 S} + \frac{R_P}{1/2\rho U^2 S} \Leftrightarrow C_T = C_F + C_P \quad (3)$$

where ρ is fluid density, U is the ship speed and S is the wetted surface area of the hull.

Alternatively, C_T can be decomposed into equivalent flat plate frictional resistance C_{F0} and residuary resistance C_R:

$$C_T = C_{F0} + C_R \quad (4)$$

Equation 4 embodies the decomposition of ship resistance as initially proposed by William Froude in 1872–1874 (Larsson and Raven 2010b). Frictional resistance C_{F0} is traditionally expressed as a function of inertia and viscosity, ie what is known today as the Reynolds number Re, representing purely frictional resistance of an equivalent flat plate, where 'equivalent' means a flat plate with the same waterline length and wetted surface area as the ship or ship's model. The residuary component C_R is expressed as a function of inertia and gravitational forces, ie Froude number Fr, as it is assumed to be predominantly composed of wave-making resistance. However, C_R also

contains *Re*-dependent viscous components, so a third way of decomposing ship resistance was called for, separating wave-making resistance C_W from the viscous component C_V (Larsson and Raven 2010b):

$$C_T = C_V(Re) + C_W(Fr). \tag{5}$$

Wave-making is assumed to be exclusively dependent on inertia and gravitational forces (Froude number), meaning that C_W can be assumed to have the same value at both model scale and full ship scale, provided that $Fr_m = Fr_s$ and that William Froude's assumption on similarity of wave patterns holds (Larsson and Raven 2010c).

The viscous resistance coefficient C_V can be further expressed as the sum of flat plate resistance C_{F0}, form effect on friction C_{FF} and form effect on pressure C_{VP} (Larsson and Raven 2010b):

$$C_T = (C_{F0} + C_{FF} + C_{VP}) + C_W \tag{6}$$

Form effects C_{FF} and C_{VP} arise from differences between the flat plate friction line C_{F0} and the hull's viscous resistance C_V, due to two simultaneous mechanisms: (1) increased friction on the hull (tangential force), denoted by C_{FF}, arises from the displacement of streamlines around the hull, resulting in increased speed near the hull as compared to the flow around the flat plate, and (2) increased pressure resistance on the hull (normal force), denoted by C_{VP} and referred to as viscous pressure, arises from the boundary layer development along the length of the hull, which causes streamline displacement from the hull in the aft body, thus decreasing the pressure at the aft body and leading to increased resistance (Lackenby 1962; Larsson and Raven 2010b).

In practice, form effects can be obtained from running a model in the towing tank at sufficiently low speed, since $C_W \to 0$ as $Fr \to 0$ (Larsson and Raven 2010c), or running CFD simulations without a free-surface ($C_W = 0$), also known as single-phase or double-body simulations (Kouh et al. 2009). Form factors are then defined as (Nagamatsu 1980):

$$K_F = \frac{C_F}{C_{F0}} - 1 \tag{7}$$

$$K_P = \frac{C_{VP}}{C_{F0}} \tag{8}$$

where C_F is the hull friction coefficient, as in Equation 3. Ship resistance can be finally expressed as a function of the form factors K_F and K_P, flat plate friction C_{F0} and wave-making resistance C_W:

$$C_T = \left(1 + K_F + K_P\right) C_{F0} + C_W \tag{9}$$

or, using a single form factor $K = K_F + K_P$:

$$C_T = (1 + K)\, C_{F0} + C_W \tag{10}$$

Form factors are Reynolds-dependent and scale dependent (Garcia-Gomez 2000; Kouh et al. 2009), as will be further discussed in this paper.

The effects of roughness at ship scale can be expressed in terms of increased resistance ΔC_T, representing the change in force required to tow the ship. Schultz (2007) uses Granville's similarity law scaling, which makes use of a roughness function ΔU^+ (as in Equation 1) in order to determine the change in flat plate frictional resistance ΔC_{F0}. The final formula for total ship resistance is given as (Schultz 2007; modified after Gillmer and Johnson 1982):

$$C_{T,s} = C_{F0,s} + C_R + \Delta C_{F0,s} + C_A \tag{11}$$

where C_R includes wave-making resistance and other forces acting normal to the hull, as derived directly from model-scale tests at $Fr_m = Fr_s$. For a smooth hull, the frictional coefficient $C_{F0,s}$ is obtained from friction lines, eg ITTC-57 friction line (ITTC 2011). The ITTC-57 friction line for $C_{F0,s}$ is a not a 'pure' flat plate friction line, since it already includes ~12% form factor (Larsson and Raven 2010c). Finally, a constant correlation allowance, C_A, accounts for form effects not included in the previous coefficients, among other corrections required for the scaling-up of model results obtained in a towing tank (Gillmer and Johnson 1982; Woo et al. 1983).

The decomposition of ship resistance in Equation 11 (Schultz 2007; modified after Gillmer and Johnson 1982) differs somewhat from the ITTC – International Towing Tank Conference 1978 procedure, revised in 2014 (ITTC 2014), here deliberately excluding the air resistance coefficient (only hydrodynamic resistance is considered):

$$C_{T,s} = (1 + K)C_{F0,s} + C_W + (\Delta C_{T,ITTC} + C_{A,ITTC}) \tag{12}$$

where C_W is substituted for C_R, the form factor K is introduced, and a different method is used for determining the hull roughness allowance $\Delta C_{T,ITTC}$, in this case the Townsin's formula (ITTC 2014):

$$\Delta C_{T,ITTC} = 0.044\left[\left(\frac{k_t}{L}\right)^{\frac{1}{3}} - 10Re^{-\frac{1}{3}}\right] + 0.000125 \tag{13}$$

Additionally, the revised ITTC-78 procedure includes a Reynolds-dependent correlation allowance $C_{A,ITTC}$ (Equation 12), which results in a value of $(\Delta C_{T,ITTC} + C_{A,ITTC})$ approximate to that obtained using Bowden's formula, as in the original 1978 procedure (ITTC 2014). It should be noted that Equation 13 is only valid for painted hulls with peak-to-valley roughness height $k_t < 230$ μm (over a 50-mm length).

For biofouling, methods based on the hydrodynamic equivalent sand-roughness height, k_s, have been proposed by several authors to give more accurate predictions of resistance penalty, provided that previous experimental data on biofouling roughness types (ΔU^+) are available. Such scaling-up methods include Granville's similarity law scaling (Schultz 2007) and CFD approaches (Eça et al. 2010; Eça and Hoekstra 2011; Demirel et al. 2017). Today, where the Granville method takes about 1/10 of a second to compute on a laptop computer, viscous simulations using CFD can take up to several days to run, thus limiting the number of cases that can be evaluated using CFD. Still, the Granville method has the limitation of not taking hull form effects into account, as roughness penalties are calculated on a flat plate rather than the hull shape.

The hypothesis put forward in the current study is that cost-effective flat plate calculations, such as the Granville's scaling method (Schultz 2007), could be made more accurate by multiplying roughness effects by the form factor $(1+K)$. This hypothesis is equivalent to adding the roughness effect, $\Delta C_{F0,s}$, directly to the flat plate friction line, $C_{F0,s}$:

$$C_{T,s} = (1 + K)(C_{F0,s} + \Delta C_{F0,s}) + C_W \qquad (14)$$

Thus, assuming that the effect of hull roughness on the ship's wave pattern is negligible (ie no effect on C_W), Equation 14 would mean a global roughness penalty on ship resistance given by:

$$\Delta C_{T,s} = (1 + K)\Delta C_{F0,s} \qquad (15)$$

In this paper, this hypothesis is analysed in light of recent developments on the validity of the form factor approach, and tested by re-analysing publicly available CFD results on the KRISO containership hull (KCS hull) and the equivalent flat plate (Demirel et al. 2017), as further detailed below.

Materials and methods

Repository data

CFD results re-analysed in this study are credited to Demirel et al. (2017). Simulation results from Demirel et al. (2017) are publicly available on the University of Strathclyde data repository, corresponding to full-scale towing resistance solutions for the KCS hull, separated into frictional (C_F) and normal forces (C_P). The results were obtained by Demirel et al. (2017) using a finite volume solver for the unsteady RANS equations (Reynolds-averaged Navier–Stokes equations). Resistance results for the equivalent flat plate, composed only of the frictional component C_F, were instead directly gathered from the paper (Demirel et al. 2017, tables 9 and 10), as they were not available from the repository. Simulated full-scale cases correspond to vessel speeds of 19 knots ($Re_s = 2.29 \times 10^9$) and 24 knots ($Re_s = 2.89 \times 10^9$). Other vessel specifications for the KCS hull are presented in Table 1. The full scale ship has never been built, but complete experimental model data, as well as model-scale simulations, are available for this hull geometry (Kim et al. 2001; NMRI 2017). For the KCS hull, wave-making resistance corresponds to 16% and 29% of the total resistance, at speeds of 19 and 24 knots, respectively.

Table 1. Vessel specifications for the full-scale KRISO containership (KCS) hull (Demirel et al. 2017).

Parameter	Value
Waterline length, L	232.5 m
Breadth, B	32.2 m
Design draft, T	10.8 m
Block coefficient, C_B	0.6505
Wetter surface area, S	9,498 m^2
Design speed, U	24 knots
Design Froude number, Fr	0.26

In Demirel et al. (2017), the same turbulence model was used for both hull and flat plate, corresponding to the SST (shear stress transport) k-ω turbulence model. It should be noted that modelling of the wall roughness requires a tailored near-wall mesh resolution for each hull fouling condition, as to obtain the correct non-dimensional distance between the first node and the wall, which should be higher than 30 viscous units and higher than k_s^+ (Eça and Hoekstra 2011; Demirel et al. 2014). More details on the grids used, as well as other numerical settings, can be found in the original study (Demirel et al. 2017).

Seven roughness hull conditions were tested by Demirel et al. (2017), representing both coated and fouled hull conditions that can be observed on ships' hulls (Table 2). The selected k_s values were obtained from Schultz (2007). It should be borne in mind that these values might not be representative of the diversity of fouled hull conditions for each fouling rating (Schultz 2007). Finally, it is important to note that Demirel et al. (2017) used a modified roughness function (Demirel et al. 2014), and not the original Nikuradse's roughness function for uniformly packed sand grains (Nikuradse 1933; Cebeci and Bradshaw 1977). The modified roughness function should better capture the transitionally rough behaviour of the flow over hull roughness (Demirel et al. 2014).

Form factor and wave-making resistance

Previous studies have reported dependency of the form factor K on Reynolds number (Garcia-Gomez 2000; Kouh et al. 2009). However, since in Demirel et al. (2017) the Reynolds number varies only within the full scale ($Re_s = 2.29–2.89 \times 10^9$), present analyses rely on a

Table 2. Hull roughness conditions (Schultz 2007).

Hull condition	NSTM rating	k_s (μm)	k_t (μm)
Hydraulically smooth surface	0	0	0
Typical as applied AF coating	0	30	150
Deteriorated coating or light slime	10–20	100	300
Heavy slime	30	300	600
Small calcareous fouling or weed	40–60	1,000	1,000
Medium calcareous fouling	70–80	3,000	3,000
Heavy calcareous fouling	90–100	10,000	10,000

AF = antifouling; NSTM = Naval Ships' Technical Manual (NSTM 2006).

constant form factor of $K = 0.1$, as previously reported for the KCS hull (Castro et al. 2011; Demirel et al. 2017). A double-body simulation on the KCS hull geometry would enable the form factor K to be determined more accurately for each speed, directly from the comparison between hull resistance without a free surface ($C_W = 0$) and numerical flat plate resistance (Raven et al. 2008; Kouh et al. 2009). However this was not conducted by Demirel et al. (2017).

From Equation 10, the KCS hull's wave-making resistance coefficient can be obtained as:

$$C_W = C_T - (1 + K)\, C_{F0} \tag{16}$$

The above equation differs from Equation 15 of Demirel et al. (2017), in that the flat plate's C_{F0} is used here instead of the KCS hull's friction coefficient C_F, which is related to C_{F0} by the frictional form factor K_F, ie $C_F = (1 + K_F)C_{F0}$. The current approach is therefore more consistent with the definition of $(1 + K)$ as the ratio between the hull's viscous resistance, $C_V = C_F + C_{VP}$, and flat plate's C_{F0}. This results in higher values of C_W, compared to the original values reported in Demirel et al. (2017).

Comparison of penalty prediction methods

Finally, different penalty calculation methods were ranked according to their accuracy, using full-scale CFD results for the KCS hull as reference (Demirel et al. 2017). These methods include the CFD results for the equivalent flat plate from Demirel et al. (2017) and own calculations using the Granville method, as described in Schultz (2007) using the roughness function given by Demirel et al. (2017). Additionally, each of these results (the CFD flat plate, and the Granville method) are further multiplied by a form factor $(1+K) = 1.1$ (Castro et al. 2011; Demirel et al. 2017), to determine whether such operation brings about any improvement in terms of accuracy.

Uncertainty estimates

Numerical uncertainties in the CFD results were reported by Demirel et al. (2017) and the numerical method was verified using the grid convergence index method based on Richardson extrapolation. Discretisation errors corresponded to ~1.6% and ~0.7%, for C_F (flat plate) and C_T (KCS hull), respectively. The discretisation errors for these coefficients, generically denoted E_{C_X}, are propagated in the current paper. Thus, the final error for ΔC_X is given by the following expression, where $X = T$, F or $F0$ is used to denote total hull resistance, frictional hull resistance or frictional flat plate resistance (respectively):

$$E_{\Delta C_X} = \sqrt{\left(E_{C_{X,rough}}\right)^2 + \left(E_{C_{X,smooth}}\right)^2} \tag{17}$$

For form factors, which involve the ratio between resistance coefficients (eg Equations 7 and 8), propagated errors are given by the following equation:

$$E_{K_X} = K_X \sqrt{\left(\frac{E_{C_1}}{C_1}\right)^2 + \left(\frac{E_{C_2}}{C_2}\right)^2} \tag{18}$$

where C_1 and C_2 are the two resistance coefficients (or change in resistance coefficient) used in calculating a generic form factor K_X, where $X = F$, P, ΔC_F or ΔC_T, is used to denote friction form factor, pressure form factor, form factor on change in frictional resistance or form factor on change in total resistance, respectively.

Additionally, Demirel et al. (2017) validated the numerical method against experimental model test data for the KCS hull (Kim et al. 2001) and the Granville method for the flat plate cases. The errors associated with resistance coefficients were proven to be within 2.3%.

Results and discussion

Friction form factor, K_F

From the available KCS hull and flat plate CFD results, the friction form factor K_F can be readily obtained using Equation 7, where C_F is obtained from the KCS hull and C_{F0} from the equivalent flat plate (Table 3). An approximately constant value of $K_F \sim 0.05$ is observed, with some dependency on k_s (probably due to changes in the numerical grid for different roughness height, since the tailored near-wall mesh is not currently accounted for in the uncertainty estimates), and also with a general increase with speed. The later increase with speed is in agreement with the findings of Kouh et al. (2009), where a linear increase in K with Reynolds number was observed.

The question that follows is whether a similar form effect on friction can be observed also on the change in frictional resistance due to roughness, ie a form factor on $\Delta C_F = (C_{F,rough} - C_{F,smooth})$. Results are presented in Table 4 for ΔC_F (KCS) and ΔC_{F0} (flat plate), for each rough hull condition (k_s = 30–10,000 μm), using the smooth case as a reference. Similar to the total friction (Table 3), the

Table 3. Friction and pressure form factors (K_F and K_P, respectively) obtained from published CFD results on the KRISO containership hull (KCS) and equivalent flat plate (Demirel et al. 2017), assuming $K = K_F + K_P = 0.1$ (Castro et al. 2011). Uncertainties correspond to propagated numerical discretisation errors from the original simulations.

U [knots]	k_s [μm]	$C_F \times 10^3$ (KCS)	$C_{F0} \times 10^3$ (flat plate)	$K_F = C_F / C_{F0} - 1$	$K_P = K - K_F$
19	0	1.452 ± 0.011	1.386 ± 0.022	0.048 ± 0.001	0.052
	30	1.560 ± 0.012	1.485 ± 0.023	0.050 ± 0.001	0.050
	100	1.835 ± 0.014	1.750 ± 0.027	0.048 ± 0.001	0.052
	300	2.115 ± 0.016	2.022 ± 0.032	0.046 ± 0.001	0.054
	1,000	2.509 ± 0.019	2.401 ± 0.037	0.045 ± 0.001	0.055
	3,000	3.007 ± 0.022	2.886 ± 0.045	0.042 ± 0.001	0.058
	10,000	3.734 ± 0.028	3.578 ± 0.056	0.044 ± 0.001	0.056
Average				0.046 ± 0.002	0.054
24	0	1.422 ± 0.011	1.351 ± 0.021	0.052 ± 0.001	0.048
	30	1.577 ± 0.012	1.496 ± 0.023	0.054 ± 0.001	0.046
	100	1.840 ± 0.014	1.750 ± 0.027	0.052 ± 0.001	0.048
	300	2.121 ± 0.016	2.022 ± 0.032	0.049 ± 0.001	0.051
	1,000	2.515 ± 0.019	2.401 ± 0.037	0.047 ± 0.001	0.053
	3,000	3.015 ± 0.022	2.886 ± 0.045	0.045 ± 0.001	0.055
	10,000	3.742 ± 0.028	3.571 ± 0.056	0.048 ± 0.001	0.052
Average				0.050 ± 0.002	0.050

Table 4. Form factor $K_{\Delta CF}$ on the change in friction due to hull roughness, as obtained from published CFD results on the KRISO containership hull (KCS) and equivalent flat plate (Demirel et al. 2017). Uncertainties correspond to propagated numerical discretisation errors from the original simulations.

U [knots]	k_s [μm]	$\Delta C_F \times 10^3$(KCS)	$\Delta C_{F0} \times 10^3$(flat plate)	$K_{\Delta CF} = \Delta C_F / \Delta C_{F0}$ - 1
19	30	0.108 ± 0.016	0.099 ± 0.032	0.086 ± 0.030
	100	0.382 ± 0.017	0.364 ± 0.035	0.051 ± 0.005
	300	0.663 ± 0.019	0.636 ± 0.038	0.042 ± 0.003
	1,000	1.057 ± 0.021	1.015 ± 0.043	0.041 ± 0.002
	3,000	1.555 ± 0.025	1.500 ± 0.050	0.037 ± 0.001
	10,000	2.282 ± 0.030	2.192 ± 0.060	0.041 ± 0.001
Average				0.050 ± 0.031
24	30	0.156 ± 0.016	0.145 ± 0.031	0.073 ± 0.018
	100	0.419 ± 0.017	0.399 ± 0.034	0.049 ± 0.005
	300	0.699 ± 0.019	0.671 ± 0.038	0.042 ± 0.003
	1,000	1.093 ± 0.021	1.050 ± 0.043	0.041 ± 0.002
	3,000	1.593 ± 0.025	1.535 ± 0.050	0.038 ± 0.001
	10,000	2.320 ± 0.030	2.220 ± 0.060	0.045 ± 0.001
Average				0.048 ± 0.019

change in the KCS hull's frictional resistance coefficient is always higher than that of the equivalent flat plate, with $K_{\Delta CF}$ values of ~ 0.05 (Table 4). The propagated error is higher for $K_{\Delta CF}$ (Table 4) compared to K_F (Table 3), which is due to larger relative uncertainties in ΔC_F and ΔC_{F0} at low k_s values. However, the average $K_{\Delta CF}$ values (Table 4) are not significantly different from those obtained for K_F (Table 3), thus suggesting that the same form effect applies to both frictional resistance and the friction penalty due to hull roughness/fouling, at both speeds (19 and 24 knots).

Pressure form factor, K_P

The pressure form factor K_P is the difference between the overall form factor K and friction form factor K_F (Equations 9 and 10). In Table 3, a value $K = 0.1$ was assumed (Castro et al. 2011), since the K could not be directly determined from simulation results (double-body simulations would be required; Raven et al. 2008). Consequently, the K_P values in Table 3 should be analysed with caution, as these depend on a K value from a different source and unknown uncertainty. However, these results appear to suggest that form effects on viscous pressure are comparable to form effects on friction.

Form effect on ΔC_T

The hypothesis that the hull form can affect the resistance penalty due to biofouling is summarised by Equation 15: the change in total resistance due to hull roughness at the ship scale ($\Delta C_{T,s}$) is proportional to the change in frictional resistance of the equivalent flat plate ($\Delta C_{F0,s}$) by an overall form factor (1+K). This hypothesis is tested by comparing ΔC_T (KCS hull) to ΔC_{F0} (flat plate), as presented in Table 5 and Figure 2. The corresponding form factor, $K_{\Delta CT}$, is presented in Table 5.

It is observed that, for the lower speed of 19 knots, ΔC_T (KCS hull) is always larger than ΔC_{F0} (flat plate), with a form factor of 0.058 ± 0.025 (average value ± propagated discretisation error). This is in good agreement with the hypothesis of an overall form effect on hull roughness/biofouling penalties. Additionally, $K_{\Delta CT}$ = 0.058 ± 0.025 appears to agree with an overall form factor of K = 0.1 (Castro et al. 2011), suggesting approximately the same form effect on both full-scale resistance and hull roughness penalties. However, the hypothesis is not supported by the results at a higher speed of 24 knots, where $K_{\Delta CT}$ is approximately null (–0.012 ± 0.012). The same can be observed in Figure 2, where significant differences between the KCS hull and the flat plate (ie form effects) are only observed for the lower speed of 19 knots. Some other effect seems to cancel out the form effect on friction that was previously described. Therefore, further decomposition of

Table 5. Form factor $K_{\Delta CT}$ on change in total resistance due to hull roughness, as obtained from published CFD results on the KRISO containership hull (KCS) and equivalent flat plate (Demirel et al. 2017). Uncertainties correspond to propagated numerical discretisation errors from the original simulations.

U [knots]	k_s [μm]	$\Delta C_T \times 10^3$ (KCS)	$\Delta C_{F0} \times 10^3$ (flat plate)	$K_{\Delta CT} = \Delta C_T / \Delta C_{F0} - 1$
19	30	0.106 ± 0.019	0.099 ± 0.032	0.066 ± 0.024
	100	0.381 ± 0.021	0.364 ± 0.035	0.046 ± 0.005
	300	0.665 ± 0.023	0.636 ± 0.038	0.046 ± 0.003
	1,000	1.070 ± 0.025	1.015 ± 0.043	0.054 ± 0.003
	3,000	1.587 ± 0.028	1.500 ± 0.050	0.058 ± 0.002
	10,000	2.362 ± 0.034	2.192 ± 0.060	0.077 ± 0.002
Average				0.058 ± 0.025
24	30	0.150 ± 0.023	0.145 ± 0.031	0.037 ± 0.010
	100	0.379 ± 0.024	0.399 ± 0.034	−0.051 ± 0.005
	300	0.646 ± 0.026	0.671 ± 0.038	−0.038 ± 0.003
	1,000	1.023 ± 0.028	1.050 ± 0.043	−0.026 ± 0.001
	3,000	1.522 ± 0.031	1.535 ± 0.050	−0.009 ± 0.0003
	10,000	2.256 ± 0.036	2.220 ± 0.060	0.016 ± 0.001
Average				−0.012 ± 0.012

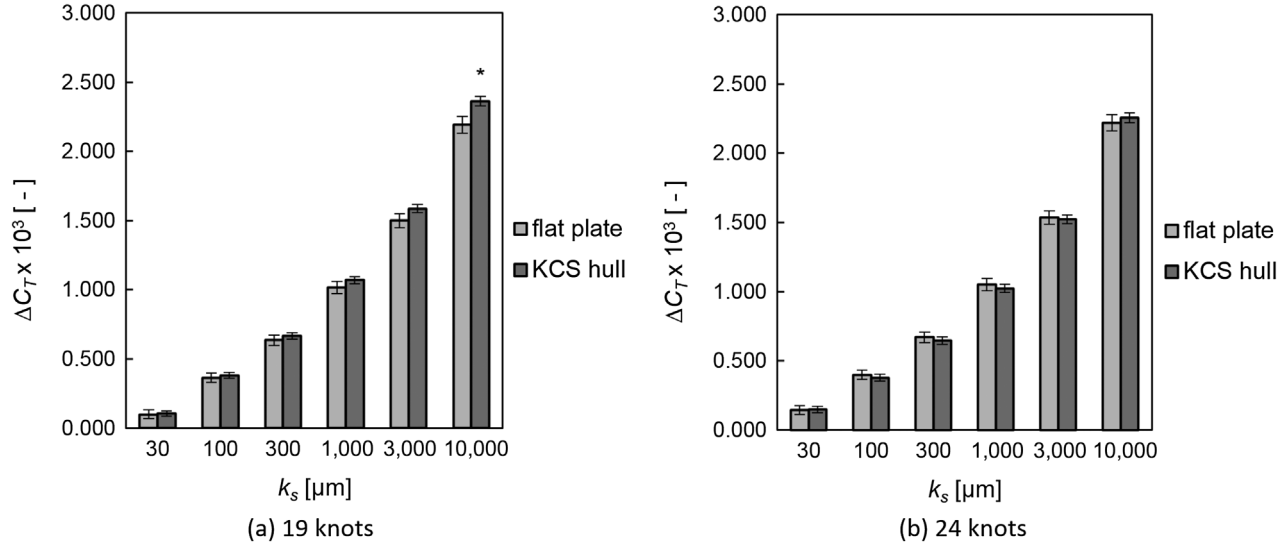

Figure 2. Hull roughness effect on resistance, ΔC_T, for the KRISO containership (KCS). (a) 19 knots, $Re_s = 2.29 \times 10^9$, (b) 24 knots, $Re_s = 2.89 \times 10^9$. Error bars correspond to propagated discretisation error of resistance coefficients C_T (KCS hull) and C_F (flat plate). Original data from Demirel et al. (2017). *Significant difference, based on numerical discretisation error.

resistance is called for, by taking into account wave-making resistance, considering that Demirel et al. (2017) reported significant changes in wave-making by an increase in hull roughness. Although the later finding is against the traditional view that wave-making resistance is not affected by hull roughness (Woods Hole Oceanographic Institute 1952), the findings by Demirel et al. (2017) agree well with other numerical studies that demonstrated viscous effects on wave patterns, namely that the boundary layer thickness (which is increased by hull roughness) changes the stern pressure field, leading to dampening of the stern wave system (Raven et al. 2008; Larsson and Raven 2010b, p. 35–36).

Wave-making resistance

The wave-making resistance coefficient C_W was obtained using Equation 16 and the results are presented in Table 6.

Significant changes in C_W as a function of hull roughness k_s were noted: for 19 knots, C_W is 18% lower for a heavily fouled hull compared to the smooth hull, whereas for 24 knots C_W was up to 30% lower. It should also be noted that C_W obtained in this study was higher than previously reported in Demirel et al. (2017), as Equation 16 uses the flat plate C_{F0} instead of the KCS hull C_F. Thus, whereas previously reported C_W values corresponded to 0.060–0.208 $\times 10^{-3}$ for 19 knots, and 0.237–0.534 $\times 10^{-3}$ for 24 knots (Demirel et al. 2017), these values correspond now to 0.231–0.281 $\times 10^{-3}$ and 0.425–0.611 $\times 10^{-3}$, for 19 and 24 knots respectively (Table 6). Also, it is noted that, for each speed, the change in C_W due to hull roughness is not as strong as previously reported in Demirel et al. (2017), where changes corresponded to −56% and −72%, for 19 and 24 knots, respectively.

In Table 6, the expected viscous form effects on the flat plate roughness penalty, $K \times \Delta C_{F0}$, is also presented for comparison with ΔC_W. Interestingly, at a speed of 19 knots, the negative change in C_W is not sufficient to overcome the positive form effect, where the sum $K \times \Delta C_{F0} + \Delta C_W$ is positive and increases with hull roughness (Table 6, 19 knots), explaining the form factor $K_{\Delta CT} = 0.058 \pm 0.012$ at 19 knots (Table 5). For 24 knots, the negative change in C_W is much higher than at 19 knots and cancels out the positive form effect, so that the sum $K \times \Delta C_{F0} + \Delta C_W$ is close to null (Table 6, 24 knots), explaining the approximately null form factor $K_{\Delta CT}$ at 24 knots (Table 5). Thus, the hypothesis of a form factor affecting hull penalties due to roughness (Equation 15) cannot be generalised for all speeds, since the effect of hull roughness on wave pattern cannot be neglected.

Table 6. Wave-making resistance C_W, and form effect on flat plate hull roughness penalty $K \times \Delta C_{F0}$, as obtained from published CFD results on the KRISO containership hull (KCS) and equivalent flat plate (Demirel et al. 2017), using $K = 0.1$ (Castro et al. 2011).

U [knots]	k_s [μm]	$C_W \times 10^3$	$\Delta C_W \times 10^3$		$K \times \Delta C_{F0} \times 10^3$ (flat plate)	$(K \times \Delta C_{F0} + \Delta C_W) \times 10^3$
19	0	0.281				
	30	0.278	−0.003	(−1%)	0.010	0.007
	100	0.261	−0.020	(−7%)	0.036	0.017
	300	0.247	−0.034	(−12%)	0.064	0.029
	1,000	0.234	−0.047	(−17%)	0.102	0.055
	3,000	0.218	−0.063	(−22%)	0.150	0.087
	10,000	0.231	−0.050	(−18%)	0.219	0.170
24	0	0.611				
	30	0.602	−0.009	(−1%)	0.015	0.005
	100	0.551	−0.060	(−10%)	0.040	−0.020
	300	0.519	−0.092	(−15%)	0.067	−0.025
	1,000	0.479	−0.132	(−22%)	0.105	−0.027
	3,000	0.445	−0.167	(−27%)	0.154	−0.013
	10,000	0.425	−0.186	(−30%)	0.222	0.036

Comparison of penalty prediction methods

Using as a reference the full-scale CFD results for the KCS hull, alternative methods for predicting the rough hull penalty are compared here. These methods are: (1) CFD results for the equivalent flat plate, and (2) the Granville method for the equivalent flat plate. Each of these flat-plate methods is also multiplied by the form factor $(1 + K)$ for comparison. The results are presented in Figure 3.

For 19 knots ($Re_s = 2.29 \times 10^9$), the CFD flat plate results (Figure 3a, 'flat CFD') underestimate the effect of roughness on the KCS hull by as much as 4–7%, as expected from previous analyses (Table 5, 19 knots: $K_{\Delta CT} = 0.058 \pm 0.012$). The results from the Granville method underestimate ΔC_T by 17% for $k_s = 30$ μm, but are within −4% to +0.2% of the KCS hull reference for all other hull conditions. Multiplication of CFD flat plate results by $(1+K)$ leads to a smaller error, with 2–5% overestimation, while applying $(1+K)$ to the results of the Granville method generally leads to worse results, with −8% to +10% differences relative to the KCS hull. Overall, for 19 knots, the methods are ranked as follows, in order of decreasing agreement with the KCS hull results: (1) CFD flat plate results multiplied by $1 + K$, (2) the CFD flat plate results, (3) the Granville method, and (4) the Granville method multiplied by $1 + K$.

For 24 knots ($Re_s = 2.89 \times 10^9$), the CFD flat plate results (Figure 3b, 'flat CFD') show errors relative to the KCS hull between −4% and +5%. Results from the Granville method show errors between −19% and +8%. Multiplication of CFD flat plate results by $(1 + K)$ leads to an overestimation of as much as 6% to 16%, while applying $(1 + K)$ to Granville method results leads to errors of between −11% and +19%. Overall, for 24 knots, the methods are ranked as follows, in order of decreasing agreement with KCS hull results: (1) the CFD flat plate results, (2) the CFD flat plate

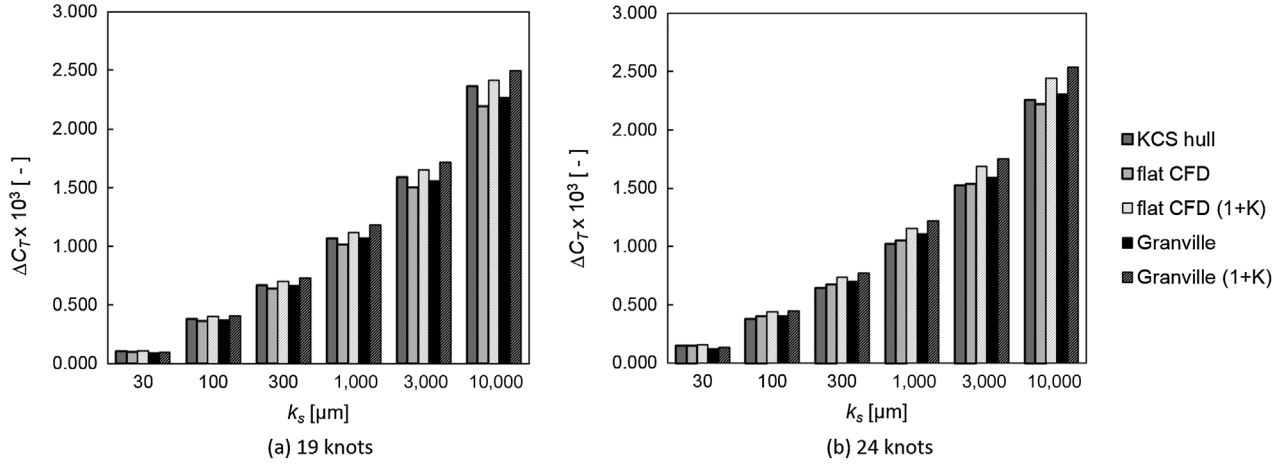

Figure 3. Comparison of hull roughness penalty prediction methods for the KRISO containership (KCS). (a) 19 knots, $Re_s = 2.29 \times 10^9$, (b) 24 knots, $Re_s = 2.89 \times 10^9$. Original data from Demirel et al. (2017).

results multiplied by 1+*K*, (3) the Granville method, and (4) the Granville method multiplied by 1 + *K*.

From the above results, there is no clear advantage in considering a form factor in rough hull penalty predictions. This is supported by the above observation of a significant change in wave-making resistance resulting in cancelling effects. Overall, the time-saving Granville method seems to yield reasonably accurate results, with no further improvement by considering the form factor.

Finally, it should be stressed that the method used in obtaining the form factor, including which smooth friction line is selected (Garcia-Gomez 2000), has an important impact on the results. There can be large differences in the form factor between model-scale towing tank results and the full scale (Kouh et al. 2009), which might be related to practical problems such as partially immersed bulbous bows, immersed transoms, differences in wave-breaking, Reynolds and Froude number dependency, surface tension effects and occurrence of flow separation at model scale, particularly at the low speed range used for determining the form factor at model scale (ITTC 1990). Thus, a more accurate, full-scale estimation of the form factor *K* as a function of speed should be considered in the future, eg by performing full-scale double-body CFD simulations (single phase) for the specific hull shape at different speeds of interest (Kouh et al. 2009). Also, the form factor should be determined relative to the same smooth friction line used in roughness penalty predictions (Schoenherr friction line in the Granville method, according to Schultz 2007), to obtain consistent results (Garcia-Gomez 2000). However, the present conclusions obtained with a form factor of $K = 0.1$ (Castro et al. 2011) should not change significantly, since the form factor is not expected to vary widely within the full-scale range of Reynolds number investigated ($2.29–2.89 \times 10^9$).

Considering the above, rapid calculation procedures used in economic and environmental assessment of the impact of hull roughness (eg the Granville method) should avoid using the form factor approach as initially hypothesised in this study, at least on vessels with significant wave-making resistance (≥29%), as an incorrect form effect might significantly compromise the accuracy of predicted hull roughness penalties on calm-water resistance. Nevertheless, since positive $K_{\Delta CT}$ values could be obtained at lower speed for the KRISO containership (Table 5), future studies should investigate further whether the form factor approach of Equation 15 holds for vessels with a lower percentage of wave-making resistance (≤16%), and also for vessels with a higher form factor than the KRISO containership, such as tankers.

Conclusions

Form effects on ship resistance arise from flow differences between a ship's hull and the equivalent flat plate (same length and wetted surface area), leading to higher friction and pressure resistance on the hull. Since some methods for predicting penalties due to hull roughness/biofouling make use of flat plate models, eg the Granville method, it was hypothesised that similar form effects on flat plate resistance would also be observed on hull resistance penalties due to biofouling.

Re-analysis of CFD results from a previous study on the KRISO containership and the equivalent flat plate, at varying hull roughness height (Demirel et al. 2017), show form effects at the lower speed of 19 knots, with $K_{\Delta CT} = 0.058 \pm 0.012$, which however vanish at the higher speed of 24 knots. This is currently attributed to cancelling effects from the traditionally overlooked hull roughness effect on wave-making resistance, which is more significant at a vessel speed of 24 knots, compared to 19 knots. However, additional evidence of roughness effects on wave-making resistance should be gathered in future studies, particularly by experimental fluid dynamics.

Considering the current results, the application of a form effect into flat-plate predictions on hull roughness penalties is discouraged, although it might still be valid at low vessel speeds. Future work should further consider cases with low wave-making resistance (≤16% of total resistance) and also for vessels with a higher form factor. The form factor should preferably be determined for each speed, using full-scale double-body CFD simulations (single phase) and referring to the same smooth friction line used in roughness penalty predictions.

Nomenclature

B	ship's breadth
C	smooth wall log-law intercept
C_B	block coefficient, $C_B = \nabla/(LBT)$
C_A	correlation allowance (constant)
$C_{A,ITTC}$	Reynolds number-dependent correlation allowance (ITTC 2014)
C_F	resistance coefficient, $C_F=R_F / (½\rho U^2 S)$
C_{F0}	flat plate resistance coefficient, $C_{F0}=R_{F0} / (½\rho U^2 S)$
C_{FF}	form effect on frictional resistance coefficient, $C_{FF}=R_{FF} / (½\rho U^2 S)$
C_P	pressure resistance coefficient, $C_P=R_P / (½\rho U^2 S)$
C_R	residuary resistance coefficient, $C_R=R_R / (½\rho U^2 S)$
C_T	total resistance coefficient, $C_T=R_T / (½\rho U^2 S)$

C_V	viscous resistance coefficient, $C_V=R_V / (½\rho U^2 S)$
C_{VP}	viscous pressure resistance coefficient, $C_{VP}=R_{VP} / (½\rho U^2 S)$
C_W	wave-making resistance coefficient, $C_W=R_W / (½\rho U^2 S)$
ΔC_{F0}	change in flat plate resistance coefficient due to hull roughness/fouling
ΔC_T	change in total resistance coefficient due to hull roughness/fouling
E	uncertainty
Fr	Froude number, $Fr = U / (g\,L)^{½}$
g	gravitational acceleration = 9.81 m s^{-2}
k_s	equivalent uniform sand roughness height (fully rough regime)
k_t	peak-to-valley roughness height, based on line measurements along 0.05 m
K	form factor, $K = C_V/C_{F0} - 1 = K_F + K_P$
K_F	form factor on friction, $K_F = C_F/C_{F0}$ - 1
K_P	form factor on pressure, $K_P = C_{VP}/C_{F0}$
$K_{\Delta CF}$	form factor on the change in friction due to hull roughness, $K_{\Delta CF} = \Delta C_F/\Delta C_{F0} - 1$
$K_{\Delta CT}$	form factor on resistance penalty due to hull roughness, $K_{\Delta CT} = \Delta C_T/\Delta C_{F0} - 1$
L	waterline length
R_F	frictional resistance
R_{F0}	flat plate frictional resistance
R_{FF}	form effect on frictional resistance
R_P	pressure resistance
R_R	residuary resistance
R_T	total towing resistance, $R_T = R_F + R_P = R_{F0} + R_R = R_V + R_W$
R_V	viscous resistance
R_{VP}	form effect on pressure resistance (viscous pressure)
R_W	wave-making resistance
Re	Reynolds number, $Re = U\,L / \nu$
S	wetted surface area
T	ship's draft
U	ship or model speed through water
u_τ	wall shear velocity, $u_\tau = (\tau_w / \rho)^{½}$
ΔU^+	roughness function
∇	volumetric ship displacement
ε	wall origin error
κ	von Kármán constant
ν	kinematic viscosity of the fluid
ρ	density of the fluid
τ_w	wall shear stress

Superscript

+	inner-scaling of a variable, using u_τ for velocity scale or ν/u_τ for length scale

Subscripts

F	hull friction
F0	flat plate friction
m	model scale
s	full ship scale (or equivalent sand roughness)
P	hull pressure resistance
T	total

Acknowledgements

The authors would like to acknowledge Professor Rickard Bensow (Chalmers University of Technology), for interesting discussions and comments on an earlier version of the manuscript, and Superintendent Lars-Olof Albert, for valuable and encouraging discussions, and for generously allowing access to the full dry-docking process of a merchant vessel. The contribution of three anonymous reviewers to this paper is acknowledged.

Disclosure statement

No potential conflict of interest was reported by the authors.

Funding

The ongoing project on biofouling is supported by the Swedish Energy Agency [grant number 2014-004848]; additional funding to Ann I Larsson was provided by the Swedish Research Council FORMAS [grant number 215-2012-1134].

ORCID

Dinis Oliveira http://orcid.org/0000-0001-8948-6884
Ann I. Larsson http://orcid.org/0000-0003-3268-2037
Lena Granhag http://orcid.org/0000-0002-0340-7469

References

Andersen P, Borrod A-S, Blanchot H. 2005. Evaluation of the service performance of Ships. Mar Technol. 42:177–183.

Bradshaw P. 2000. A note on "critical roughness height" and "transitional roughness". Physics of Fluids. 12:1611. doi:10.1063/1.870410

Candries M, Atlar M. 2005. Experimental investigation of the turbulent boundary layer of surfaces coated with marine antifoulings. J Fluids Eng. 127:219. doi:10.1115/1.1891148

Castro AM, Carrica PM, Stern F. 2011. Full scale self-propulsion computations using discretized propeller for the KRISO container ship KCS. Comput Fluids. 51:35–47. doi:10.1016/j.compfluid.2011.07.005

Cebeci T, Bradshaw P. 1977. Momentum transfer in boundary layers. New York (NY): Hemisphere Publishing Corporation / McGraw-Hill Book Company.

Demirel YK, Khorasanchi M, Turan O, Incecik A, Schultz MP. 2014. A CFD model for the frictional resistance prediction of antifouling coatings. Ocean Eng. 89:21–31. doi:10.1016/j.oceaneng.2014.07.017

Demirel YK, Turan O, Incecik A. 2017. Predicting the effect of biofouling on ship resistance using CFD. Appl Ocean Res. 62:100–118. doi:10.1016/j.apor.2016.12.003

Eça L, Hoekstra M. 2011. Numerical aspects of including wall roughness effects in the SST k-omega eddy-viscosity turbulence model. Comput Fluids. 40:299–314.

Eça L, Hoekstra M, Raven HC. 2010. Quantifying roughness effects by ship viscous flow calculations. In: Purtell LP, Reed A, Beck R, Larsson L, Lee CS, Rhee KP, Gharib M, editors. 28th Symp Nav Hydrodyn. Pasadena, California: Marin - Maritime Research Institute Netherlands; p. 12–17.

Garcia-Gomez A. 2000. On the form factor scale effect. Ocean Eng. 27:97–109. doi:10.1016/S0029-8018(98)00042-0

Gillmer T, Johnson B. 1982. Introduction to naval architecture. Annapolis, MD: US Naval Institute. doi:10.1007/978-94-011-6039-1

Grigson C. 1987. Full-scale viscous drag of actual ship surfaces and the effect of quality of roughness on predicted power. J Ship Res. 31:189–206.

ICS. 2017. Shipping and World Trade. Int Chamb Shipp Website [Internet]. [accessed 2017 Nov 13]. http://www.ics-shipping.org/shipping-facts/shipping-and-world-trade

IMO. 2014. Reduction of GHG emissions from ships - Third IMO GHG Study 2014 - Final Report. MEPC 67/INF3.

ISO. 2016. ISO 19030:2016 - Ships and marine technology - Measurement of changes in hull and propeller performance. ISO/TC 8/SC 2.

ITTC. 1990. 19th ITTC Report of the Powering Performance Committee.

ITTC. 2011. The 1978 ITTC Performance Prediction Method. 26th Int Towing Tank Conf.

ITTC. 2014. Recommended Procedures and Guidelines - 1978 ITTC performance prediction method 7.5-02-03-01.4 (Revision 03).

Johansson L-E. 1984. The local effect of hull roughness on skin friction. RINA Trans. 127:187–201.

Kim WJ, Van SH, Kim DH. 2001. Measurement of flows around modern commercial ship models. Exp Fluids. 31:567–578. doi:10.1007/s003480100332

Kouh J-S, Chen Y-J, Chau S-W. 2009. Numerical study on scale effect of form factor. Ocean Eng. 36:403–413. doi:10.1016/j.oceaneng.2009.01.011

Lackenby H. 1962. Resistance of ships, with special reference to skin friction and hull surface condition. Proc Inst Mech Eng. 176:981–1014. doi:10.1243/PIME_PROC_1962_176_077_02

Larsson L, Raven HC. 2010a. The flow around the hull and the viscous resistance. In: Paulling JR, editor. The principles of naval architecture series – ship resistance and flow. Jersey City (NJ): The Society of Naval Architects and Marine Engineers; p. 51–77.

Larsson L, Raven HC. 2010b. Decomposition of resistance. In: Paulling JR, editor. The principles of naval architecture series – ship resistance and flow. Jersey City (NJ): The Society of Naval Architects and Marine Engineers; p. 13–16.

Larsson L, Raven HC. 2010c. Experimental resistance prediction and flow measurement. In: Paulling JR, editor. The principles of naval architecture series - ship resistance and flow. Jersey City (NJ): The Society of Naval Architects and Marine Engineers; p. 98–107.

Leer-Andersen M, Larsson L. 2003. An experimental/numerical approach for evaluating skin friction on full-scale ships with surface roughness. J Mar Sci Technol. 8:26–36.

Lewthwaite JC, Molland AF, Thomas KW. 1984. An investigation into the variation of ship skin frictional resistance with fouling. RINA Trans. 127:269–284.

Monty JP, Dogan E, Hanson R, Scardino AJ, Ganapathisubramani B, Hutchins N. 2016. An assessment of the ship drag penalty arising from light calcareous tubeworm fouling. Biofouling. 32:451–464. doi:10.1080/08927014.2016.1148140

Munk T, Kane D, Yebra DM. 2009. The effects of corrosion and fouling on the performance of ocean-going vessels: a naval architectural perspective. In: Advances in marine antifouling coatings and technologies. Oxford: Woodhead Publishing Limited; p. 148–176.

Nagamatsu T. 1980. Calculation of viscous pressure resistance of ships based on a higher order boundary layer theory. J Soc Nav Archit Japan. 1980:20–34. doi:10.2534/jjasnaoe1968.1980.20

Nikuradse J. 1933. Strömungsgesetze in rauhen Rohren [Laws of flow in rough pipes]. Forschungsheft 361 [translated as National Advisory Committee for Aeronautics, 1950, Technical Memorandum 1292]. Göttingen (DE): Verein Deutscher Ingenieure - Verlag.

NMRI. 2017. Tokyo 2015: a workshop on CFD in ship hydrodynamics - KRISO Container Ship (KCS) [Internet] [accessed 2017 Oct 11]. http://www.t2015.nmri.go.jp/kcs.html.

NSTM. 2006. Chapter 081 – Water-borne underwater hull cleaning of Navy ships. Washington DC.

Raven HC, Van Der Ploeg A, Starke AR, Eça L. 2008. Towards a CFD-based prediction of ship performance - progress in predicting full-scale resistance and scale effects. Trans R Inst Nav Archit Part A Int J Marit Eng. 150:31–42.

Schultz MP. 2004. Frictional resistance of antifouling coating systems. J Fluids Eng. 126:1039. doi:10.1115/1.1845552

Schultz MP. 2007. Effects of coating roughness and biofouling on ship resistance and powering. Biofouling. 23:331–341. doi:10.1080/08927010701461974

Schultz MP, Bendick JA, Holm ER, Hertel WM. 2011. Economic impact of biofouling on a naval surface ship. Biofouling. 27:87–98. doi:10.1080/08927014.2010.542809

Walker JM. 2014. The application of wall similarity techniques to determine wall shear velocity in smooth and rough wall turbulent boundary layers. J Fluids Eng. 136:051204(1)–051204(10).

Woo EL, Karafiath G, Borda G. 1983. Ship-model correlation of powering performance on USS Oliver Hazard Perry, FFG-7 Class. Mar Technol. 20:35–52.

Woods Hole Oceanographic Institute. 1952. Marine fouling and its prevention. Menasha, WI: George Banta Publishing Co.